

Method for determining the optical constants of thin dielectric films with variable thickness using only their shrunk reflection spectra

J J Ruíz-Pérez¹, J M González-Leal², D A Minkov³ and E Márquez²

¹ Real Instituto y Observatorio de la Armada, 11110—San Fernando (Cádiz), Spain

² Departamento de Física de la Materia Condensada, Facultad de Ciencias, Universidad de Cádiz, 11510—Puerto Real (Cádiz), Spain

³ Research Institute for Fracture Technology, Tohoku University, Sendai, Japan

E-mail: emilio.marquez@uca.es

Received 20 February 2001, in final form 1 June 2001

Published 7 August 2001

Online at stacks.iop.org/JPhysD/34/2489

Abstract

Thickness inhomogeneities in thin films have a large influence on their optical transmission and reflection spectra. If not taken into account, this may lead to rather large calculated values for the absorption coefficient or the erroneous presence of an absorption-band tail, as well as to significant errors in the calculated values of the refractive index and the film thickness. The effect of thickness variation on the optical reflection spectrum of a thin dielectric film covering a thick non-absorbing substrate, is analysed in detail in this paper, and analytical expressions are presented for such a reflection spectrum and its upper and lower envelopes. A method is suggested for determining the refractive index $n(\lambda)$ and the extinction coefficient $k(\lambda)$, as well as the average thickness and the thickness variation, of a thin dielectric film with variable thickness, by using only the two envelopes of the corresponding shrunk reflection spectrum. This method is used for the geometrical and optical characterization of thermally-evaporated amorphous chalcogenide films, deposited on glass substrates.

1. Introduction

The optical properties of thin dielectric films have been investigated thoroughly during the last decades [1–4]. Thin-film thickness inhomogeneities such as wedge shaping and surface roughness have also been studied, but mostly when the transmission spectrum is utilized [5–7]. In this paper we present formulae for the reflection spectrum of a thin dielectric film with variable thickness covering a thick non-absorbing substrate, as well as its top and bottom envelopes. The effect of the thickness variation on the interference fringes of the reflection spectrum is analysed in detail, and a method is presented for calculating the optical constants $n(\lambda)$ and $k(\lambda)$, the average thickness \bar{t} , and the thickness variation Δt , of a non-uniform thin dielectric film, only from the corresponding shrunk reflection spectrum that otherwise would have been useless. It is shown that the errors made

in the computation of the above film characteristics, are limited within 1%, when this method is employed. The algorithm of the calculations has been successfully applied for the geometrical and optical characterization of thermally-evaporated amorphous chalcogenide films, deposited on glass substrates.

2. Assumptions and formulation of the method

The proposed method for the geometrical and optical characterization of thin dielectric films with variable thickness, is based mainly on the following assumptions.

- (i) A thin isotropic dielectric layer covers a thick non-absorbing substrate, and this optical system is immersed in air.
- (ii) Radiation of mean wavelength λ and spectral half-width $\Delta\lambda$, is normally incident on the sample.

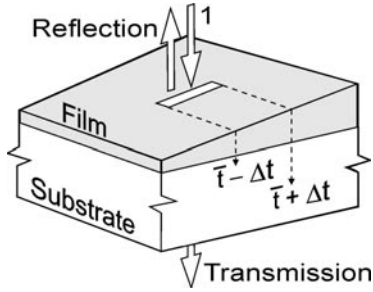


Figure 1. Sketch of a wedge-shaped thin film on a thick transparent substrate. The illuminated area is illustrated by a white rectangle positioned in the central region of the film. The radiation is incident normally to the sample.

- (iii) Interference of internally-reflected radiation occurs in the thin film ($\Delta\lambda \ll \lambda^2/(2nt)$), and is negligible in the substrate ($\Delta\lambda \gg \lambda^2/(2st_s)$), where n and t are the refractive index and the thickness of the film, respectively, and s and t_s are the corresponding parameters for the substrate.
- (iv) The refractive index of the film is larger than the refractive index of the substrate, i.e. $n > s$.
- (v) The film is weakly absorbing in the studied spectral region, i.e. $n^2 \gg k^2$ and $s^2 \gg k^2$, where k is the extinction coefficient of the film.

It has been shown in [8,9], that when the above assumptions are satisfied, and the thickness of the dielectric film is uniform, the reflectance of such a two-layer optical system is expressed as follows:

$$R = \frac{(ad)^2 + (bcx)^2 - 2abcdx \cos(\phi)}{(bd)^2 + (acx)^2 - 2abcdx \cos(\phi)} + \frac{gx^2}{(bd)^2 + (acx)^2 - 2abcdx \cos(\phi)} \times \frac{1}{b^3 f + a^3 ex^2 - 2abcdx \cos(\phi)} \quad (1)$$

where

$$\begin{aligned} a &= n - 1 & b &= n + 1 & c &= n - s & d &= n + s \\ e &= n - s^2 & f &= n + s^2 & g &= 64s(s - 1)^2 n^4 \\ x &= \exp(-\alpha t) & \phi &= 4\pi n t / \lambda & \alpha &= 4\pi k / \lambda. \end{aligned}$$

The formula for the reflectance of this system, when the dielectric film is non-uniform, can be derived from (1). If the thickness varies linearly over the film surface, this thickness can be considered to change within the interval $[\bar{t} - \Delta t, \bar{t} + \Delta t]$, over the illuminated area, as shown in figure 1. The reflection spectrum has to be measured in such a way that the same area is illuminated at all wavelengths. In this case Δt can be considered to be independent of the wavelength. It is important to note that similarly to [5], the theory developed in this paper is also valid when some irregularities occur periodically over the illuminated area, in the form of surface roughness. Hence, the analytical expression for the reflectance of this particular optical system, is obtained by integrating equation (1) over t . However, this is prohibitively difficult analytically, because x depends on t , and an acceptable approximation is to consider x to equal its average value over the range of integration with

respect to t , $[\bar{t} - \Delta t, \bar{t} + \Delta t]$. This approximation is an excellent one when $\Delta t \ll \bar{t}$. The optical absorbance x is then redefined as $x = \exp(-\alpha \bar{t})$, and the integration of equation (1) with respect to t (or equivalently, ϕ) gives place to:

$$R_{\Delta t} \approx \frac{1}{\phi_2 - \phi_1} \int_{\phi_1}^{\phi_2} R d\phi \quad (2)$$

where the integration boundaries are $\phi_1 = 4\pi n(\bar{t} - \Delta t)/\lambda$ and $\phi_2 = 4\pi n(\bar{t} + \Delta t)/\lambda$.

Solving the integral from (2) gives the following analytical expression for the reflectance:

$$\begin{aligned} R_{\Delta t} &= 1 - \frac{1}{\theta(L_1 - L_0)} \\ &\times \left\{ \frac{gx^2}{L_3 L_4} \left[\tan^{-1} \left(\frac{L_3}{L_4} L_9 \right) - \tan^{-1} \left(\frac{L_3}{L_4} L_8 \right) \right] \right. \\ &+ \frac{(L_0 - L_5)(L_1 - L_0) - gx^2}{L_6 L_7} \\ &\left. \times \left[\tan^{-1} \left(\frac{L_6}{L_7} L_9 \right) - \tan^{-1} \left(\frac{L_6}{L_7} L_8 \right) \right] \right\} \quad (3) \end{aligned}$$

where the following auxiliary variables are used

$$\begin{aligned} \theta &= 4\pi n \Delta t / \lambda & L_0 &= b^2 d^2 + a^2 c^2 x^2 \\ L_1 &= b^3 f + a^3 ex^2 & L_2 &= 2abcdx \\ L_3 &= (L_2 + L_1)^{1/2} & L_4 &= (L_1 - L_2)^{1/2} \\ L_5 &= a^2 d^2 + b^2 c^2 x^2 & L_6 &= (L_0 + L_2)^{1/2} \\ L_7 &= (L_0 - L_2)^{1/2} & L_8 &= \tan(\phi_1/2) \\ L_9 &= \tan(\phi_2/2). \end{aligned}$$

Equation (3) is valid for each wavelength λ , from the spectral region of medium absorption to transparency.

To illustrate the theory presented here, three films with the following geometrical and optical characteristics are considered.

- (i) Average thickness of the films, $\bar{t} = 1000$ nm.
- (ii) Wedging parameter, $\Delta t = 0, 20$ and 40 nm.
- (iii) Refractive index of the films, $n(\lambda) = 2.6 + (3 \times 10^5 / \lambda^2)$ (λ in nm).
- (iv) Extinction coefficient of the films, $k(\lambda) = (\lambda / 4\pi) \times 10^{[(1.5 \times 10^6 / \lambda^2) - 8]}$ (λ in nm).
- (v) Refractive index of the substrate, $s = 1.51$ (constant).
- (vi) Wavelength, $\lambda = 500 \div 900$ nm.

The above values of $n(\lambda)$ and $k(\lambda)$ represent typical values of α -Si:H [5, 8].

It has been shown in [5] that increasing the wedging parameter Δt , results in increased shrinking of the transmission spectrum of a wedge-shaped thin dielectric layer on a thick transparent substrate. The analogy between the mathematical formulation of the transmittance and reflectance of such an optical system, indicates that increasing Δt should also lead to increased shrinking of the reflection spectrum. Unfortunately, the $\tan^{-1}[\dots \tan[\dots]]$ functions introduce discontinuities around the maxima of the reflection spectrum $R_{\Delta t}$, calculated from equation (3), which are similar to the discontinuities formulated in [5] for the corresponding transmission spectrum. Reflection spectra $R_{\Delta t}$, plotted

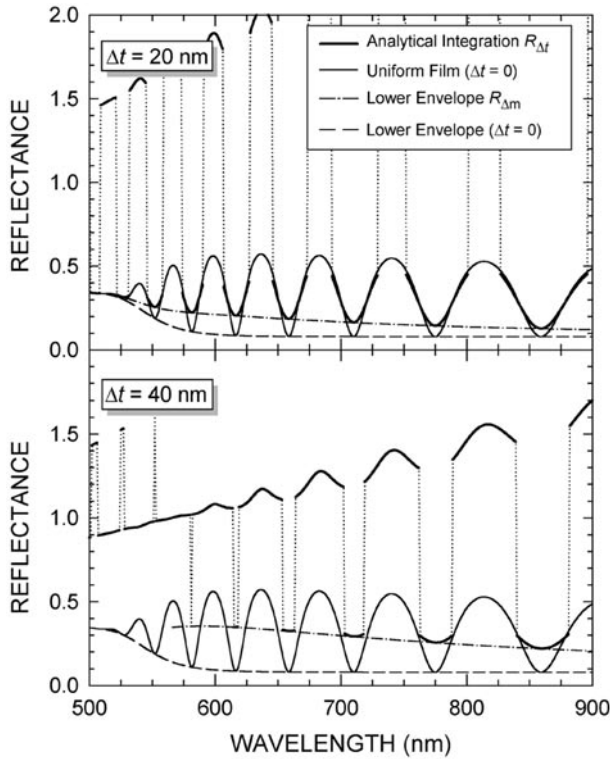


Figure 2. Calculated reflection spectra $R_{\Delta t}$ and their lower envelopes $R_{\Delta m}$ for three α -Si:H films on a glass substrate, with the geometrical and optical characteristics presented in items (i)–(vi).

from (3), with the geometrical and optical characteristics given above (see (i)–(vi)), are presented in figure 2. It is seen that the simulated spectra, for $\Delta t = 20$ and 40 nm, have reasonable values of the reflectance, $0 \leq R_{\Delta t} \leq 1$, only around the minima, and this usable region decreases with increasing Δt .

The analytical expression for the lower envelope can be obtained, taking into account that the tangent points λ_{tan} between the reflection spectrum and its two envelopes, are characterized by the dependence [5]:

$$2n\bar{t} = m\lambda_{tan} \quad (4)$$

where the order number m is an integer for λ_{tan} from the lower envelope of the reflection spectrum, $R_{\Delta m}$, and half-integer for λ_{tan} from the upper envelope, $R_{\Delta M}$. Then, the auxiliary variables L_8 and L_9 can be rewritten as follows:

$$\begin{aligned} L_8 &= \tan\left(\frac{\phi_1}{2}\right) = \tan\left(\frac{2\pi n(\bar{t} - \Delta t)}{\lambda}\right) \\ &= \tan\left(\pi m\left(1 - \frac{\Delta t}{\bar{t}}\right)\right) = -\tan\left(\frac{2\pi n\Delta t}{\lambda}\right) \\ &= -\tan\left(\frac{\theta}{2}\right) \\ L_9 &= \tan\left(\frac{\phi_2}{2}\right) = \tan\left(\frac{2\pi n(\bar{t} + \Delta t)}{\lambda}\right) \\ &= \tan\left(\pi m\left(1 + \frac{\Delta t}{\bar{t}}\right)\right) = +\tan\left(\frac{2\pi n\Delta t}{\lambda}\right) \\ &= +\tan\left(\frac{\theta}{2}\right). \end{aligned} \quad (5)$$

The substitution of L_8 and L_9 from (5) into equation (3) gives an analytical expression for the lower envelope:

$$\begin{aligned} R_{\Delta m} &= 1 - \frac{2}{\theta(L_1 - L_0)} \left\{ \frac{gx^2}{L_3L_4} \tan^{-1}\left(\frac{L_3}{L_4}L_{10}\right) \right. \\ &\quad \left. + \frac{(L_0 - L_5)(L_1 - L_0) - gx^2}{L_6L_7} \tan^{-1}\left(\frac{L_6}{L_7}L_{10}\right) \right\} \quad (6) \end{aligned}$$

where $L_{10} = \tan(\theta/2)$. The lower envelopes corresponding to the reflection spectra $R_{\Delta t}$ shown in figure 2, are also plotted in this figure.

As mentioned before, the reflection spectra calculated from (3) have erroneous values, $R_{\Delta t} > 1$, around all the maxima of the spectra for $\Delta t = 20$ and 40 nm. Correspondingly, the following auxiliary function

$$\begin{aligned} R_\pi &= \frac{(ad)^2 + (bcx)^2 + 2abcdx \cos(\phi)}{(bd)^2 + (acx)^2 + 2abcdx \cos(\phi)} \\ &\quad + \frac{gx^2}{(bd)^2 + (acx)^2 + 2abcdx \cos(\phi)} \\ &\quad \times \frac{1}{b^3f + a^3ex^2 + 2abcdx \cos(\phi)} \quad (7) \end{aligned}$$

is used to derive the analytical expression for the upper envelope of the spectrum, $R_{\Delta M}$, instead of (1). This new function is obtained by a phase shift of π radians of the function R from (1), and has the very useful property that its maxima/minima, are positioned at the same wavelengths as the corresponding minima/maxima of the function R . Furthermore, R_π replaces R in (2), and the result of its analytical integration

$$\begin{aligned} R_{\pi\Delta t} &\approx \frac{1}{\phi_2 - \phi_1} \int_{\phi_1}^{\phi_2} R_\pi d\phi = 1 - \frac{1}{\theta(L_1 - L_0)} \left\{ \frac{gx^2}{L_3L_4} \right. \\ &\quad \times \left[\tan^{-1}\left(\frac{L_4}{L_3}L_9\right) - \tan^{-1}\left(\frac{L_4}{L_3}L_8\right) \right] \\ &\quad + \frac{(L_0 - L_5)(L_1 - L_0) - gx^2}{L_6L_7} \\ &\quad \left. \times \left[\tan^{-1}\left(\frac{L_7}{L_6}L_9\right) - \tan^{-1}\left(\frac{L_7}{L_6}L_8\right) \right] \right\} \quad (8) \end{aligned}$$

is similar to the reflection spectrum $R_{\Delta t}$, calculated from (1).

The reflection spectra $R_{\pi\Delta t}$ are simulated from (8), using all the geometrical and optical characteristics given above (see (i)–(vi)). These reflection spectra are presented in figure 3. It can be seen that, for $\Delta t = 20$ and 40 nm, the simulated spectra have reasonable values of the reflectance, $0 \leq R_{\pi\Delta t} \leq 1$, only around the maxima of the spectra and, similarly to $R_{\Delta t}$, the usable region decreases with increasing Δt .

Following the procedure for deriving the lower envelope by (6), the upper envelope of the reflection spectrum, $R_{\Delta M}$, is expressed as follows

$$\begin{aligned} R_{\Delta M} &= 1 - \frac{2}{\theta(L_1 - L_0)} \left[\frac{gx^2}{L_3L_4} \tan^{-1}\left(\frac{L_4}{L_3}L_{10}\right) \right. \\ &\quad \left. + \frac{(L_0 - L_5)(L_1 - L_0) - gx^2}{L_6L_7} \tan^{-1}\left(\frac{L_7}{L_6}L_{10}\right) \right]. \quad (9) \end{aligned}$$

On the other hand, the upper envelopes corresponding to the reflection spectra $R_{\pi\Delta t}$ shown in figure 3, are also plotted in this figure.

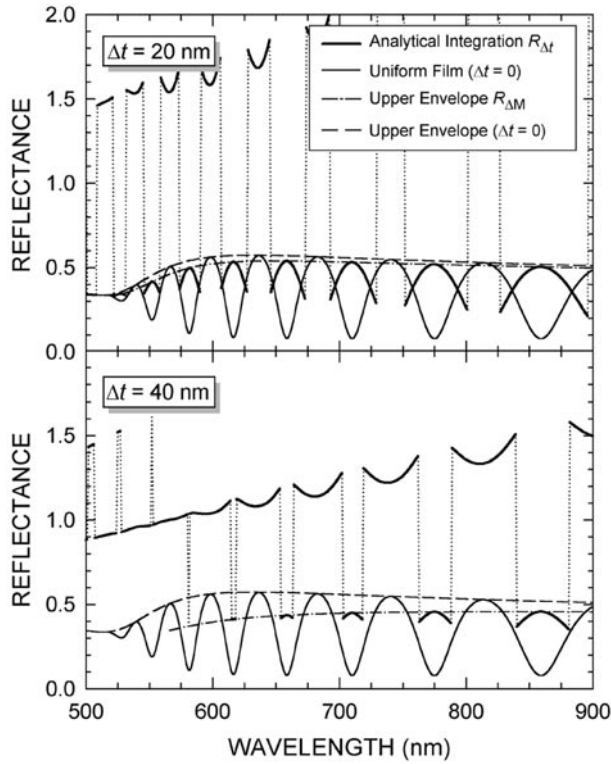


Figure 3. Calculated reflection spectra $R_{\pi \Delta t}$ and their upper envelopes $R_{\Delta M}$ for three α -Si:H films on a glass substrate, with $\Delta t = 0, 20$ and 40 nm.

Equations (6) and (9) represent a system of two transcendental equations for every wavelength λ , from the spectral region of medium absorption to transparency, which can be expressed in the following implicit form:

$$R_{\Delta M} = R_{\Delta M}(n, x, \Delta t) \quad R_{\Delta m} = R_{\Delta m}(n, x, \Delta t) \quad (10)$$

and its solution is used in the proposed method. The range of validity of the system of equations (10) is: $0 < \Delta t < \lambda/4n$. The reason for the upper limit in the wedging parameter, is the presence of new discontinuities in the expressions for the top and bottom envelopes. Above this limit, i.e. $\Delta t \geq \lambda/4n$, both envelopes would intersect and, therefore, $R_{\Delta M} \leq R_{\Delta m}$ [9].

Finally, it is interesting to point out that the theory presented here is, in principle, also valid for $n < s$. In such a case, the multiply-reflected beams at the surface of the substrate will be accompanied by a phase change of π radians. This would lead to a change in the relative position of the reflection spectrum of the film-on-substrate system, with respect to the reflection spectrum of the bare substrate: the latter being now above the former. In addition, the mathematical expressions of the envelopes will be exchanged, i.e. the upper envelope, $R_{\Delta M}$, would be now described by (6), rather than (9), and, therefore, the integer (instead of half-integer) order numbers would be associated with its corresponding tangent points (just contrary changes would occur in the lower envelope, $R_{\Delta m}$). However, common substrates having a high refractive index, such as silicon wafers or germanium substrates, also show high values of the extinction coefficient and, thus, it cannot be neglected, as in the case of the glass substrates.

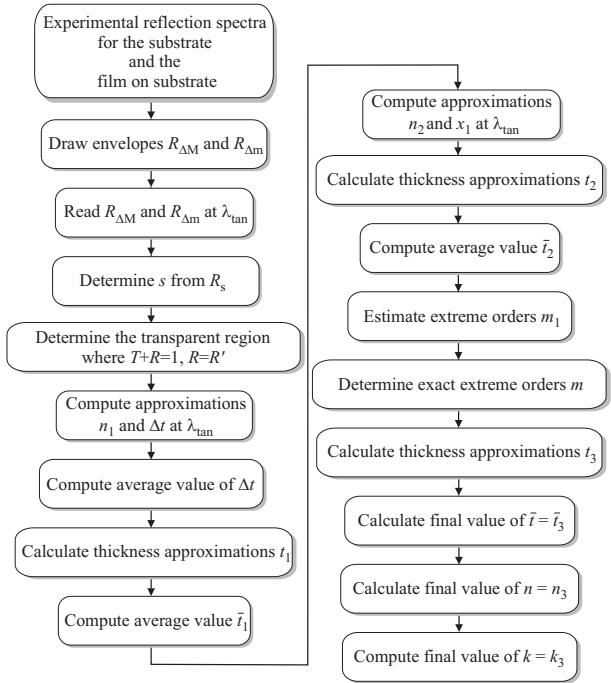


Figure 4. Block diagram of the complete algorithm for calculating \bar{t} , Δt , $n(\lambda)$ and $k(\lambda)$ of a non-uniform thin dielectric film covering a thick transparent substrate, from its corresponding shrunk reflection spectrum.

3. Algorithm of the calculation

A block diagram of the algorithm of the method for determining the spectral dependences $n(\lambda)$ and $k(\lambda)$, and the average film thickness \bar{t} and the thickness variation Δt , is presented in figure 4. The operation of the sequential steps of this algorithm is explained below. After the scanning of the experimental reflection spectrum, its two envelopes $R_{\Delta M}$ and $R_{\Delta m}$ are computer drawn by employing the very useful algorithm developed by McClain *et al* [10]. The refractive index of the substrate s is calculated independently from the reflection spectrum of the bare substrate R_s , using the following relationship [8, 9]

$$s = \frac{1 + \sqrt{R_s(2 - R_s)}}{1 - R_s}. \quad (11)$$

The present method requires that the reflection spectrum of the sample contains a spectral region where the film can be regarded as being transparent. This region can be found by measuring both the transmission and reflection spectra, and considering that $R + T = 1$, or $R = R'$, only in this particular spectral region, where T is the transmission and R' the reflection measured from the substrate side of the sample. Taking into account that $x = 1$ in the transparent region, the system of the two transcendental equations (10) can be solved for n and Δt , at every tangent point λ_{tan} between the reflection spectrum and its two envelopes. These first values of the refractive index obtained are denoted by n_1 . The final value of the wedging parameter $\bar{\Delta t}$ is determined by averaging a certain set of Δt values, as explained in the next section, and then the system (10) is solved again to obtain the next approximations n_2 and x_1 , at all λ_{tan} . The experimental errors

in $R_{\Delta M}$ and $R_{\Delta m}$ decrease notably the accuracy of these n_2 values, calculated from the system (10) [9].

If $n'_{1(2)}$ and $n''_{1(2)}$ are the refractive indices belonging to the set of n_1 (or n_2) values, at two different tangent points λ' and λ'' , and Δm is the difference of their corresponding order numbers, the thickness t_1 (or t_2) is expressed from equation (4), as follows:

$$t_{1(2)} = \frac{\Delta m}{2} \frac{\lambda' \lambda''}{(\lambda' n''_{1(2)} - \lambda'' n'_{1(2)})}. \quad (12)$$

When two alternative tangent points are used (both from the upper envelope or from the lower envelope), then $\Delta m = 1$. Hence, an initial approximate value of the thickness, \bar{t}_1 (or a new improved value \bar{t}_2), is obtained by averaging the set of t_1 (or t_2) values, calculated from (12). The order number of a given tangent point m_1 is now estimated from (4), using \bar{t}_1 (or \bar{t}_2) and the corresponding n_1 (or n_2). As mentioned before, the exact order numbers are consecutive half-integers for the upper tangent points, and consecutive integers for the lower tangent points. Therefore, the m_1 values are conveniently rounded off to their closest exact half-integer or integer order numbers, m 's.

The final average thickness of the non-uniform film \bar{t} ($=\bar{t}_3$) is obtained by averaging the values for t_3 calculated from (4), where n_1 's (or n_2 's), as well as their corresponding m 's, are used. The final value of the refractive index n ($=n_3$) is obtained, at each tangent point, from (4) by substituting \bar{t} and m . It must be indicated that when working with the reflection spectrum rather than the transmission spectrum, some more tangent points are used, which leads to a larger set of values of n , corresponding to a wider spectral range.

The final value of the extinction coefficient k can be determined from the absorbance x ($=\exp(-4\pi k \bar{t}/\lambda)$), by three different approaches: using the previously obtained x_1 values, or solving either (6) or (9) with respect to x , obtaining, respectively, x_2 and x_3 values. The best results are achieved employing the third approach, i.e. calculating the extinction coefficient k_3 from equation (9) for the upper envelope of the reflection spectrum, $R_{\Delta M}$, and using the already known values of $\bar{\Delta t}$, \bar{t} and $n(\lambda)$. It is certainly recommended not to use the lower envelope $R_{\Delta m}$ described by equation (6), because it is strongly sensitive to errors in the measured data [9].

4. Accuracy of the method

The proposed method for calculating the wedging parameter, the average thickness, the refractive index and the extinction coefficient, of a non-uniform thin dielectric film deposited on a transparent substrate, is applied to two different reflection spectra. The first one is a simulated reflection spectrum, obtained using the geometrical and optical characteristics introduced by (i)–(vi) above, and performing the integration (2) numerically with $\Delta t = 30$ nm. This reflection spectrum, and its two envelopes, $R_{\Delta M}$ and $R_{\Delta m}$, are shown in figure 5, which also includes the reflection spectrum of the bare substrate, R_s . The results obtained at the different steps of the calculation of n and k , from the top and bottom envelopes of this spectrum, are presented in table 1. The spectral region over which the reflection spectrum has been simulated, is characterized by considerable optical absorption at shorter wavelengths, therefore, the hypothesis $x = 1$, used when solving the

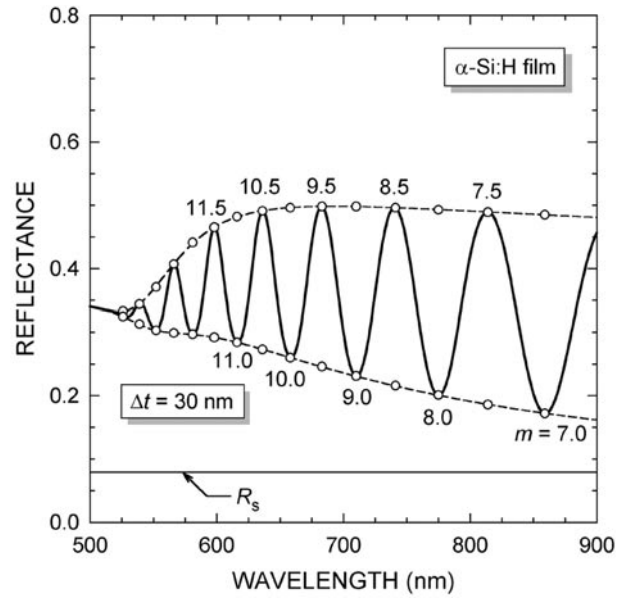


Figure 5. Simulated reflection spectrum and the top and bottom envelopes of a wedge-shaped thin film of α -Si:H with $\Delta t = 30$ nm, on a glass substrate. The reflection spectrum for the substrate alone is also plotted. The order numbers, m 's, for some tangent points have been marked.

system (10) for n and Δt , is valid only for those tangent points corresponding to longer wavelengths. This is confirmed by the less accurate values of n_1 and t_1 , which are derived from them. The last two columns of table 1 contain the true values, n_{tr} and k_{tr} , of the refractive index and the extinction coefficient of the film, respectively. It is seen that the relative error $|n - n_{tr}|/n_{tr}$ made in the calculation of the refractive index does not exceed 0.2%, and the relative error $|k - k_{tr}|/k_{tr}$ is certainly not larger than 1%. The geometrical parameters \bar{t} and Δt are also calculated with relative errors smaller than 0.5%.

It should be mentioned that the values of Δt listed in table 1, depart from the true value, $\Delta t_{tr} = 30$ nm, for shorter wavelengths, which is due to the fact that the Δt values have been calculated considering $x = 1$ in the system (10), and the computation assigns the effect of $x < 1$ to n_1 and Δt . Furthermore, it has been shown in [9] that, for larger wavelengths, the system (10) is very sensitive to x , which also leads to overestimated Δt values (see table 2, introduced below). Therefore, to study initially the list of Δt values and to average next the subset showing a low scattering, is a good practical criterion to determine accurately the final value of the wedging parameter, $\bar{\Delta t}$.

The second reflection spectrum analysed corresponds to a real amorphous chalcogenide thin film of chemical composition $As_{33}S_{67}$, deposited by thermal evaporation in vacuum on a glass substrate [11], and was obtained by a double-beam UV/Vis/NIR spectrophotometer (Perkin Elmer, model Lambda-19). The experimental reflection spectrum of this sample, its two envelopes, and the reflection spectrum of the bare substrate, are all shown in figure 6(a). To illustrate the advantage that there are some more tangent points when using the reflection spectrum, in comparison with the corresponding transmission spectrum, both experimental reflection and transmission spectra belonging to the amorphous

Table 1. Calculation of the wedging parameter, the average thickness, the refractive index and the extinction coefficient, of a hypothetical α -Si:H film, based on the proposed method. The values of λ_{tan} , $R_{\Delta M}$ and $R_{\Delta m}$ correspond to the optical reflection spectrum from figure 5. It is observed from the values of n_1 and Δt , that the hypothesis $x = 1$ is certainly not valid for the tangent points corresponding to the shorter wavelengths. Therefore, the t_1 value does not represent a good approximation of the average thickness of the film. The final value of the wedging parameter, $\overline{\Delta t}$, was calculated by averaging only the underlined Δt values. Less accurate values of t_1 and t_2 , as well as the values of k_3 and $k_{tr} < 10^{-3}$, have been omitted in the table. (True average thickness, $\bar{t}_{tr} = 1000$ nm; true wedging parameter, $\Delta t_{tr} = 30$ nm; average thickness, $\bar{t}_1 = 1037 \pm 32(3.1\%)$ nm; average thickness, $\bar{t}_2 = 998 \pm 8(0.8\%)$ nm; average thickness, $\bar{t}_3 = 1002 \pm 1(0.1\%)$ nm; calculated wedging parameter, $\overline{\Delta t} = 30.2 \pm 0.3(1.0\%)$ nm.)

λ_{tan} (nm)	$R_{\Delta M}$	$R_{\Delta m}$	n_1	Δt (nm)	t_1 (nm)	n_2	x_1	t_2 (nm)	m_1	m	t_3 (nm)	n_3	k_3	n_{tr}	k_{tr}
859	0.485	0.172	3.005	<u>30.0</u>	1007	2.999	$\simeq 1$	1003	6.99	7.0	1003	3.000	—	3.007	—
814	0.489	0.186	3.050	<u>30.0</u>	1019	3.044	$\simeq 1$	1004	7.49	7.5	1003	3.046	—	3.053	—
775	0.493	0.201	3.096	<u>30.1</u>	1024	3.092	$\simeq 1$	1005	7.99	8.0	1003	3.094	—	3.099	—
741	0.496	0.216	3.140	<u>30.1</u>	1045	3.140	$\simeq 1$	1002	8.48	8.5	1003	3.143	—	3.146	—
710	0.498	0.231	3.183	<u>30.1</u>	1089	3.186	0.997	1002	8.98	9.0	1003	3.189	—	3.195	0.001
683	0.498	0.246	3.221	<u>30.3</u>	—	3.235	0.990	1001	9.48	9.5	1003	3.238	0.001	3.243	0.001
658	0.496	0.260	3.252	<u>30.4</u>	—	3.281	0.979	1002	9.98	10.0	1003	3.283	0.001	3.293	0.002
636	0.491	0.273	3.271	<u>30.8</u>	—	3.330	0.958	1000	10.48	10.5	1003	3.332	0.002	3.342	0.003
616	0.482	0.284	3.269	31.4	—	3.379	0.922	995	10.98	11.0	1003	3.381	0.004	3.391	0.004
598	0.465	0.292	3.238	32.4	—	3.430	0.861	995	11.48	11.5	1002	3.432	0.007	3.439	0.007
581	0.441	0.297	3.171	34.0	—	3.479	0.767	998	11.99	12.0	1002	3.479	0.012	3.489	0.013
566	0.407	0.299	3.078	36.5	—	3.531	0.622	997	12.49	12.5	1002	3.530	0.021	3.536	0.022
552	0.371	0.303	2.991	39.7	—	3.582	0.433	975	12.99	13.0	1002	3.581	0.037	3.585	0.037
539	0.344	0.313	2.950	42.5	—	3.633	0.228	—	13.49	13.5	1001	3.631	0.063	3.633	0.062
526	0.333	0.325	2.963	43.5	—	3.683	0.075	—	14.02	14.0	1000	3.675	0.102	3.684	0.111

Table 2. Calculation of the wedging parameter, the average thickness, the refractive index and the extinction coefficient, of a real amorphous chalcogenide film of composition $As_{33}S_{67}$, based on the proposed method. The values of λ_{tan} , s , $R_{\Delta M}$ and $R_{\Delta m}$ correspond to the optical reflection spectra from figure 6(a). The final value of the wedging parameter, $\overline{\Delta t}$, was calculated by averaging only the underlined Δt values. Less accurate values of n_1 , t_1 , m_1 and t_3 , as well as the values of $k_3 < 10^{-3}$, have been omitted in the table. (Average thickness, $\bar{t}_1 = 1603 \pm 25(1.6\%)$ nm; average thickness, $\bar{t}_3 = 1613 \pm 6(0.4\%)$ nm; wedging parameter, $\overline{\Delta t} = 29.5 \pm 0.8(2.7\%)$ nm.)

λ_{tan} (nm)	s	$R_{\Delta M}$	$R_{\Delta m}$	n_1	Δt (nm)	t_1 (nm)	m_1	m	t_3 (nm)	n_3	k_3
2138	1.506	0.327	0.087	2.306	46.0	1615	3.46	3.5	1623	2.320	—
1873	1.506	0.328	0.087	2.309	35.3	1602	3.95	4.0	1622	2.322	—
1667	1.500	0.328	0.090	2.314	38.2	1603	4.45	4.5	1621	2.325	—
1503	1.503	0.329	0.092	2.322	36.7	1610	4.95	5.0	1618	2.330	—
1370	1.506	0.330	0.095	2.329	35.7	1611	5.45	5.5	1618	2.336	—
1259	1.508	0.330	0.098	2.336	34.7	1601	5.95	6.0	1617	2.342	—
1165	1.508	0.331	0.100	2.342	34.3	1559	6.45	6.5	1617	2.347	—
1085	1.510	0.332	0.103	2.352	33.4	1561	6.95	7.0	1615	2.354	—
1015	1.512	0.334	0.108	2.366	33.7	1605	7.47	7.5	1609	2.360	—
955	1.516	0.335	0.111	2.376	32.9	1633	7.98	8.0	1608	2.368	—
901	1.516	0.336	0.112	2.381	<u>31.2</u>	1616	8.47	8.5	1608	2.374	—
855	1.512	0.338	0.112	2.389	<u>30.1</u>	1612	8.96	9.0	1611	2.385	—
813	1.515	0.340	0.116	2.400	<u>29.6</u>	1630	9.46	9.5	1609	2.394	—
776	1.514	0.340	0.120	2.409	<u>29.9</u>	1613	9.95	10.0	1611	2.405	—
742	1.516	0.340	0.124	2.418	<u>29.9</u>	1569	10.45	10.5	1611	2.415	—
712	1.517	0.341	0.129	2.431	<u>29.8</u>	1569	10.95	11.0	1611	2.428	—
684	1.518	0.343	0.133	2.447	<u>29.7</u>	1633	11.47	11.5	1607	2.438	—
659	1.519	0.345	0.138	2.460	<u>29.5</u>	1625	11.97	12.0	1607	2.451	—
636	1.519	0.346	0.140	2.470	<u>28.9</u>	1582	12.45	12.5	1609	2.464	—
615	1.520	0.349	0.143	2.485	<u>28.3</u>	1575	12.95	13.0	1609	2.478	—
596	1.521	0.350	0.150	2.503	<u>28.5</u>	1645	13.46	13.5	1607	2.494	—
578	1.522	0.350	0.157	2.519	<u>28.9</u>	—	13.97	14.0	1606	2.508	—
562	1.522	0.351	0.162	2.531	<u>29.0</u>	—	14.44	14.5	1610	2.526	—
547	1.525	0.352	0.167	2.546	<u>28.8</u>	—	14.92	15.0	1611	2.543	—
534	1.525	0.352	0.172	2.559	<u>28.7</u>	—	15.36	15.5	1617	2.566	—
522	1.526	0.348	0.176	2.558	<u>29.0</u>	—	15.71	16.0	1633	2.589	0.001
510	1.524	0.340	0.179	—	<u>29.7</u>	—	—	16.5	—	2.608	0.002
500	1.523	0.326	0.181	—	<u>30.9</u>	—	—	17.0	—	2.635	0.004
490	1.527	0.306	0.186	—	33.1	—	—	17.5	—	2.658	0.007
481	1.528	0.282	0.192	—	36.5	—	—	18.0	—	2.684	0.013
473	1.527	0.261	0.202	—	40.3	—	—	18.5	—	2.712	0.020
465	1.527	0.247	0.214	—	43.2	—	—	19.0	—	2.739	0.027
458	1.528	0.239	0.222	—	45.0	—	—	19.5	—	2.768	0.035
448	1.530	0.238	0.234	—	45.5	—	—	20.0	—	2.777	0.036

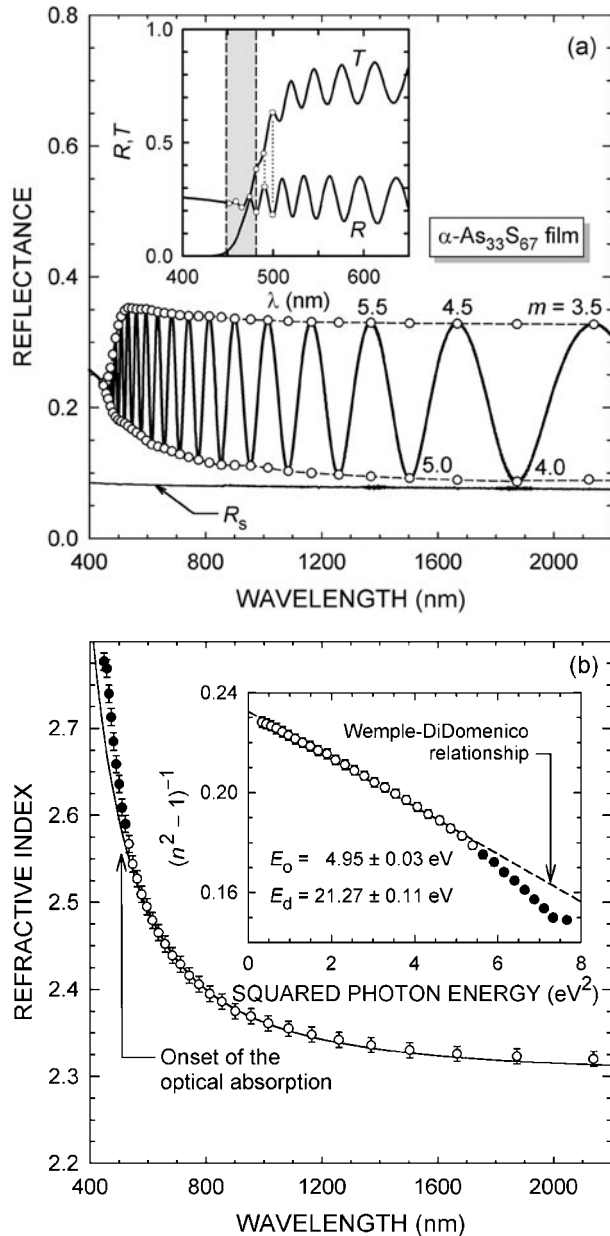


Figure 6. (a) Experimental reflection spectrum and its top and bottom envelopes for an amorphous $\text{As}_{33}\text{S}_{67}$ film covering a glass substrate. The reflection spectrum for the substrate alone is also plotted. The order numbers, m 's, for some tangent points have been marked. (b) Spectral dependence of the refractive index $n(\lambda)$ calculated from the reflection spectrum. The curve is drawn using the Wemple–DiDomenico dispersion relationship. In the inset is given a plot of the refractive-index factor $(n^2 - 1)^{-1}$ versus $(\hbar\omega)^2$, and the values obtained for the dispersion parameters, E_o and E_d , are also shown.

$\text{As}_{33}\text{S}_{67}$ film, have been plotted in the inset of figure 6(a). The results from the calculation of Δt , \bar{t} and n are presented in table 2, and the spectral dependence of the refractive index is displayed in figure 6(b). The n_2 values are not listed in table 2 because they do not improve the n_1 values, the reason being the considerable effect of the experimental errors on the resolution of system (10), with respect to n and x .

As shown in the inset of figure 6(b), in the transparent region, the final values of the refractive index can be fitted to

the Wemple–DiDomenico single-oscillator formula [12, 13]:

$$n^2(\hbar\omega) = 1 + \frac{E_o E_d}{E_o^2 - (\hbar\omega)^2} \quad (13)$$

where $\hbar\omega$ is the photon energy, E_o the single-oscillator energy and E_d the dispersion energy. On the other hand, the experimental variation in n clearly departs from that given by equation (13), at higher energies, thus, indicating the onset of the optical absorption. It must be mentioned that the proposed method was also successfully applied to several samples containing chalcogenide thin films belonging to binary systems, such as Ge–Se and Ge–S, for $400 \text{ nm} \leq \lambda \leq 2500 \text{ nm}$. In the cases investigated, the average thickness and the thickness variation were independently measured by a mechanical stylus instrument (Sloan, model Dektak 3030). These mechanically measured values differ by no more than 2% from the corresponding values calculated from the reflection spectra.

5. Conclusions

Thickness inhomogeneities in thin films cause shrinking of the optical transmission and reflection spectra. This may erroneously lead to the conclusion that an absorption-band tail exists in the long-wavelength region, and may result in serious errors in the determination of the optical constants (n , k). Correspondingly, analytical expressions are presented for the reflection spectrum of a thin dielectric film with variable thickness, covering a thick transparent substrate, as well as for the top and bottom envelopes of this spectrum. A method is suggested for the optical characterization of such a thin dielectric films utilizing these mathematical expressions. This devised method was used successfully for calculating the optical constants of thermally evaporated amorphous chalcogenide films, deposited on glass substrates. The method also allows the determination of the average thickness and the thickness variation of non-uniform films. These geometrical parameters have been independently measured by mechanical stylus instrument, and they are in excellent agreement with the corresponding data obtained from the shrunk reflection spectra.

Acknowledgments

The authors are grateful to Dr R Prieto-Alcón (Departamento de Física de la Materia Condensada, Universidad de Cádiz, Spain) for the critical reading of the paper. This work has been supported by the CICYT (Spain), under the MAT98-0791 project.

References

- [1] Arndt D P, Azzam R M A, Bennett J M, Borgogno J P, Carniglia C K, Case W E, Dobrowolski J A, Gibson U J, Tuttle Hart T, Ho F C, Hodgkin V A, Klapp W P, Macleod H A, Pelletier E, Purvis M K, Quin D M, Strome D H, Swenson R, Temple P A and Thonn T F 1984 *Appl. Opt.* **23** 3571
- [2] Heavens O S 1991 *Optical Properties of Thin Solid Films* (New York: Dover)

- [3] Ward L 1994 *The Optical Constants of Bulk Materials and Films* 2nd edn (Bristol: Institute of Physics)
- [4] Márquez E, Ramírez-Malo J B, Villares P, Jiménez-Garay R, Ewen P J S and Owen A E 1992 *J. Phys. D: Appl. Phys.* **25** 535
- [5] Swanepoel R 1984 *J. Phys. E: Sci. Instrum.* **17** 896
- [6] Márquez E, Ramírez-Malo J B, Villares P, Jiménez-Garay R and Swanepoel P 1995 *Thin Solid Films* **254** 83
- [7] Márquez E, González-Leal J M, Jiménez-Garay R, Lukic S R and Petrovic D M 1997 *J. Phys. D: Appl. Phys.* **30** 690
- [8] Minkov D 1989 *J. Phys. D: Appl. Phys.* **22** 1157
- [9] Ruiz-Pérez J J and Márquez E 1997 *Nuevos Métodos de Caracterización Óptica de Semiconductores Basados en Medidas Espectroscópicas de Reflexión* (San Fernando: Spanish Ministry of Defence)
- [10] McClain M, Feldman A, Kahaner D and Ying X 1991 *Comput. Phys.* **5** 45
- [11] Wagner T, Márquez E, Fernández-Peña J, González-Leal J M, Ewen P J S and Kasap S O 1999 *Philos. Mag. B* **79** 223
- [12] Wemple S H and DiDomenico M 1971 *Phys. Rev. B* **3** 1338
- [13] Wemple S H 1973 *Phys. Rev. B* **7** 3767